Inorganic Chemistry

pubs.acs.org/IC

Article

Living Long and Prosperous: Productive Intraligand Charge-Transfer States from a Rhenium(I) Terpyridine Photosensitizer with Enhanced Light Absorption

Ricardo Fernández-Terán* and Laurent Sévery

Cite This: https://dx.doi.org/10.1021/acs.inorgchem.0c01939

Read Online

ACCESS | Metrics & More | Article Recommendations | Supporting Information

ABSTRACT: The ground- and excited-state properties of six rhenium(I) κ^2N-tricarbonyl complexes with 4′-(4-substituted-phenyl)-terpyridine ligands bearing substituents of different electron-donating abilities were evaluated. Significant modulation of the electrochemical potentials and a nearly 4-fold variation of the triplet metal-to-ligand charge-transfer (^{3}MLCT) lifetimes were observed upon going from CN to OMe. With the more electron-donating NMe_2 group, we observed in the κ^2N complex the appearance of a very strong absorption band, red-shifted by ca. 100 nm with respect to the other complexes. This was accompanied by a dramatic enhancement of the excited-state lifetime (380 vs 1.5 ns), and a character change from ^{3}MLCT to intraligand charge transfer (^{3}ILCT), despite the remote location of the substituent. The dynamics and character of the excited states of all complexes were assigned by combining transient IR spectroscopy, IR spectroelectrochemistry, and (time-dependent) density functional theory calculations. Selected complexes were evaluated as photosensitizers for hydrogen production, with the κ^2N-NMe_2 complex resulting in a stable and efficient photocatalytic system reaching TON_{Re} values of over 2100, representing the first application of the ^{3}ILCT state of a rhenium(I) carbonyl complex in a stable photocatalytic system.

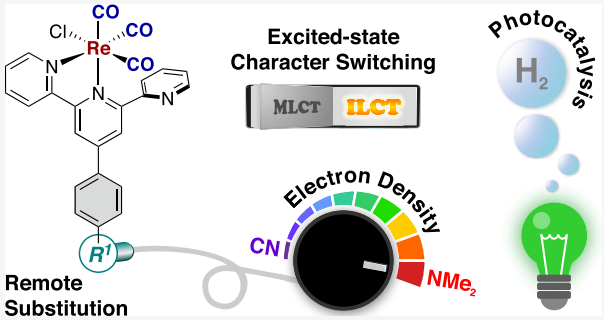

INTRODUCTION

Rhenium(I) tricarbonyl complexes bearing polypyridine ligands are very popular and well-studied molecules, especially concerning their photochemistry and photophysics. These complexes have found many applications, especially in solar energy conversion, where their use for photoelectrochemical CO_2 reduction[1−6] and as photosensitizers for hydrogen production are the most prominent ones.[7−18] The *fac*-$\{Re(CO)_3\}^+$ moiety makes these complexes excellent IR absorbers. The high sensitivity of the CO stretching modes to the electron density around the metal center, their very high IR absorption coefficients, and the overall stability of this organometallic core allowed rhenium(I) tricarbonyl complexes to become one of the most studied systems by transient IR (TRIR) spectroscopy and can be considered the closest analogues of $[Ru(bpy)_3]^{2+}$ (bpy = bipyridine) in terms of their widespread use as photosensitizers.[19,20]

Rhenium(I) tricarbonyldiimine complexes typically exhibit a purely metal-to-ligand charge-transfer (MLCT) or mixed ligand-to-ligand charge-transfer (LLCT) absorption band centered around 380 nm and the corresponding ligand-centered excitation bands at higher energies.[21] Consequently, these dyes absorb almost exclusively ultraviolet or blue light, which has prompted the design, synthesis, and study of complexes with enhanced absorption at lower energies. Most efforts in this direction have focused on the introduction of electron-withdrawing groups or the increase of conjugation of the diimine ligand framework (Figure 1A); in these cases, the absorption is red-shifted because of stabilization of the ligand-centered π^* orbitals [typically the lowest unoccupied molecular orbital (LUMO)].[22]

While the effects of substitution in the vicinity of the metal center have been previously described for rhenium(I) tricarbonyl complexes,[23−26] further understanding of the effects of substitution far away from the metal center (Figure 1B) is needed and constitutes a promising alternative to fine-tuning the properties of these complexes.

The photophysics and photochemistry of remote substituent effects in rhenium(I) complexes have been explored in the past by many groups. Among them, studies by Schanze and co-workers focused on remote substitution of the axial ligand in $[Re(bpy)(CO)_3(L)]^+$-type complexes, where the L ligand was decorated with a dimethylamino group[27] or a cation-

Received: June 30, 2020

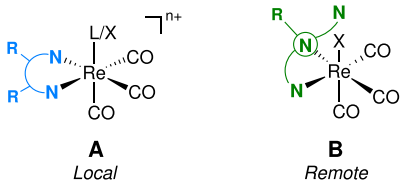

Figure 1. Different strategies for red shifting the absorption of rhenium(I) carbonyl dyes: (A) by substitution of the bpy ligands (stabilizing the ligand π^* orbitals); (B) through remote substitution, affecting the HOMO and allowing for excited-state character switching.

responsive crown macrocycle.[28] This strategy was later combined with a dipyrido[3,2-α:2′,3′-c]phenazine ligand, replacing the bpy ligand,[29] and a photoisomerizable stilbene-like moiety, as shown by Perutz and co-workers.[30] The ultrafast dynamics of intramolecular electron transfer in an azacrown-ether-decorated complex were reported by Perutz and co-workers,[31] who used transient UV−vis absorption. Similarly, porphyrin-appended rhenium(I) carbonyl complexes have been studied by ultrafast TRIR and transient UV−vis absorption spectroscopy,[32,33] and it was shown that photoexcitation of these complexes may lead to ligand dissociation.[34] In addition, the electron-transfer dynamics of porphyrin-appended rhenium(I) carbonyl complexes have been studied in NiO surfaces.[35]

Most of the examples mentioned up to now focus on substitution of the axial ligand. In our approach, we use 2,2′:6′,2″-terpyridine (terpy) to operate on the α-diimine ligand instead. The terpy framework represents an ideal structural backbone for modification by substitution. In particular, phenyl-substituted terpyridine ligands have shown remarkable photophysical and photochemical properties by themselves,[36] as well as their complexes with ruthenium(II),[37,38] platinum(II),[39] zinc(II),[40] iridium(III),[41] and other transition metals. In most of these cases, the terpyridine ligand acts as a tridentate ligand, adopting a meridional configuration around the metal center. In contrast, *fac*-rhenium(I) tricarbonyl complexes with terpyridine ligands contain a bidentate (κ^2N) terpyridine ligand in a bpy-like coordination fashion.[20,42−44]

The photophysical properties of a few rhenium-based terpyridine complexes,[45,46] as well as those with structurally related bidentate N^N ligands, have been previously studied.[47,48] Some of these evidenced long-lived intraligand charge-transfer (ILCT) states.[48]

Despite the abundant literature on terpyridine-based rhenium(I) tricarbonyl complexes, an in-depth systematic exploration of tuning of the ground- and excited-state properties is missing. Moreover, the effect of substituents in the character of the lowest excited states has only been discussed in brief. In this regard, a recent report by Shillito and co-workers showed how switching in the character of the lowest excited states (from MLCT to ILCT) frustrates tuning of the properties in rhenium(I) and platinum(II) complexes bearing triphenylamine-substituted 1,10-phenanthroline ligands.[49]

In the present work, we focus on the effect of remote substitution across the 4′-(4-R^1-phenyl)-2,2′:6′,2″-terpyridine framework on the photophysical and photochemical properties of rhenium(I) tricarbonyl complexes. We show that, in a complementary manner, as has been described before, the introduction of electron-donating substituents changes the localization of the highest occupied molecular orbital (HOMO; instead of tuning the LUMO, as shown in ref 23), leading to a change in the character of the lowest excited state from MLCT to ILCT.

We report on the synthesis, spectroscopic, crystallographic, and electrochemical characterization of a series of rhenium(I) κ^2N-tricarbonyl (**2a−2f**) complexes with substituted 4′-(4-R^1-phenyl)-2,2′:6′,2″-terpyridine ligands (**L$_a$−L$_f$**). Studying a series of complexes bearing substituents of different electron-donating abilities (from CN to NMe$_2$; Scheme 1) allowed us to correlate the observed properties with the electron density on the terpyridine ligand. The ground- and excited-state properties of these complexes were studied by UV pump−IR probe (in the femtosecond to microsecond range), electrochemistry, Fourier transform infrared (FT-IR) spectroelectrochemistry (IR-SEC) and photoluminescence measurements. In addition, through a combined experimental and computational approach, we could establish the key differences in the character of the lowest-lying excited states. Finally, we evaluated the potential utility of these complexes for photochemical energy conversion with proof-of-principle measurements of photocatalytic hydrogen evolution. To the best of our knowledge, this demonstrates for the first time the application of productive ^{3}ILCT states of rhenium(I) carbonyl complexes in photocatalysis.

RESULTS AND DISCUSSION

Synthesis and Characterization. The 4′-(4-R^1-phenyl)-2,2′:6′,2″-terpyridine ligands (**L$_a$−L$_f$**) were readily obtained in one step from 2-acetylpyridine and the corresponding 4-R^1-

Scheme 1. Synthetic Route and Structures of the Compounds Studied in the Present Work

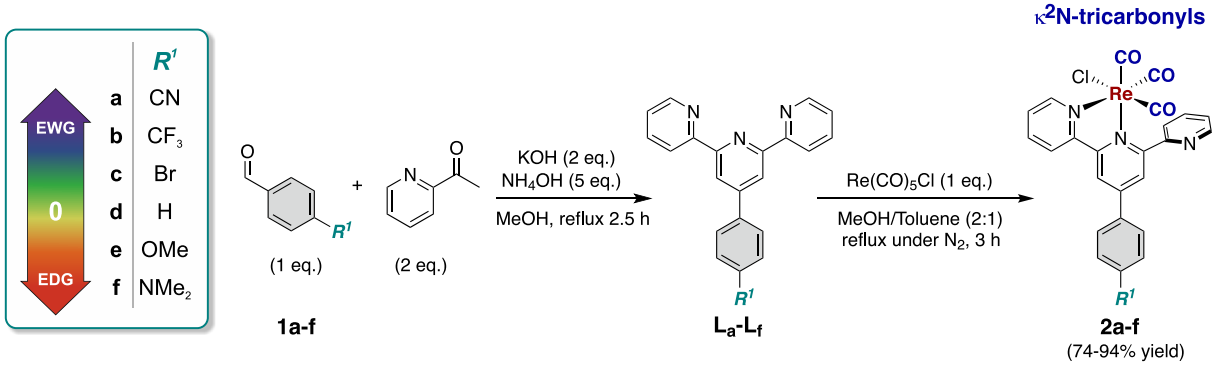

https://dx.doi.org/10.1021/acs.inorgchem.0c01939
Inorg. Chem. XXXX, XXX, XXX−XXX

benzaldehyde using a modified Kröhnke methodology, as reported previously.[50,51] This ligand framework and synthetic methodology enable easy modification at the 4′ position of the terpyridine ligand. The κ^2N-tricarbonyl complexes (**2a**–**2f**) were obtained in excellent yield from $Re^I(CO)_5Cl$ as air-stable yellow solids (**2f** as a yellow-green solid) by refluxing in a methanol/toluene mixture [see the Supporting Information (SI) for details]. Single-crystal X-ray diffraction analysis was performed for the κ^2N-tricarbonyl complexes **2a**, **2b**, and **2e**. Figure 2 shows the displacement ellipsoid plot of the structure of **2a** as a representative example.

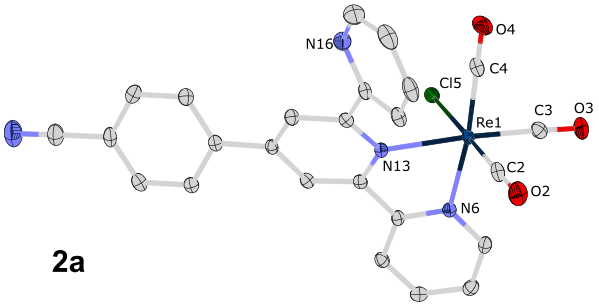

Figure 2. Displacement ellipsoid representation at the 50% probability level of the crystal structure of complex **2a**. Hydrogen atoms and solvent molecules are omitted for clarity.

The structures of the κ^2N-tricarbonyl complexes show a bpy-like coordination of the terpyridine ligand to the *fac*-$\{Re(CO)_3\}^+$ core, with the two rings being twisted by about 10°. The third pyridine ring is rotated by ca. 45–50°, and the 4′-phenyl ring is rotated by 15–25° with respect to the plane of the central pyridine ring. A brief discussion of the crystal structures and a table of crystallographic parameters are given in Table S1. In the solution ^1H NMR spectra of complexes **2a**–**2f**, we observe two sets of signals for the peripheral pyridine rings, supporting the κ^2N coordination with a dangling pyridine observed in the solid state.

Steady-State Spectroscopic Properties. The UV–vis and FT-IR spectra of **2d**–**2f** in *N*,*N*-dimethylformamide (DMF; as representative examples) are shown in Figure 3 (other spectra are provided in Figures S1 and S2 and Table S2). In the UV–vis absorption spectra of the κ^2N-tricarbonyl complexes (**2a**–**2f**), we observe a band centered around 380 nm with an extinction coefficient $\varepsilon \approx 4000$ cm^{-1} M^{-1}, typical of an MLCT band in rhenium(I) complexes.[21] The higher-energy bands are attributed to ligand-centered π–π^* transitions. Time-dependent density functional theory (TD-DFT) calculations performed in *Gaussian 09*, revision D.01,[52] nicely reproduce all of these features (Figure S3).

The MLCT absorption band shows a hypsochromic shift of ca. 720 cm^{-1} as the electron-donating character of the substituent increases from CN to OMe (values provided in Table S2). These shifts are much smaller than those obtained upon direct substitution at the 4 and 4′ positions of the bpy ligand (ca. 6250 cm^{-1} between NO_2 and NH_2)[23,53] and suggest a small, albeit observable, electronic effect of substitution in the 4′-phenyl ring of the terpy ligands upon going from CN to OMe. While the spectra of the complexes with electron-withdrawing substituents do not show significant changes, complexes with more electron-donating groups show distinct features in their UV–vis spectra. For **2e** (R^1 = OMe), we observe a new shoulder at lower energy, which evolves into a very intense absorption band in **2f**, bearing the more electron-donating $R^1 = NMe_2$ moiety. This additional low-energy band (Figure 3, red) has a significantly higher extinction coefficient than typical MLCT or even ligand-centered π–π^* transitions, providing a first hint into its different character.

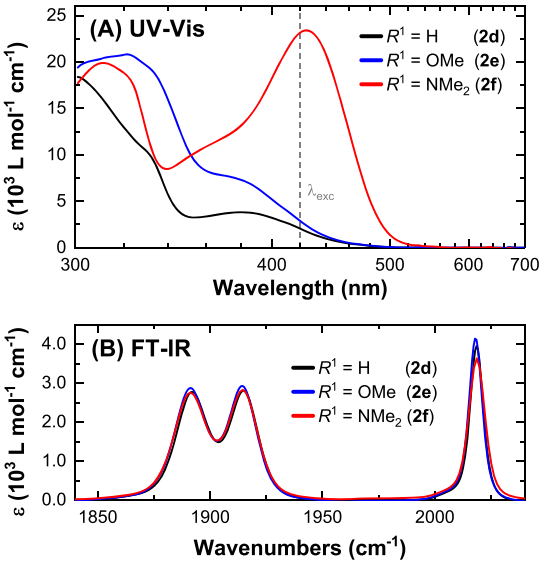

Figure 3. (A) UV–vis and (B) FT-IR spectra of **2d**–**2f** in DMF, as representative examples. The dashed line in part A indicates the excitation wavelength used in the transient absorption experiments (420 nm).

In the FT-IR absorption spectra of **2a**–**2f** in DMF, we observe the typical features of the *fac*-$\{Re(CO)_3\}^+$ moiety: three strong ν_{CO} bands at ca. 2019, 1915, and 1892 cm^{-1}, corresponding to modes of A′(1), A″, and A′(2) symmetries, respectively. The ν_{CO} frequencies shift only 2–4 cm^{-1} (Table S2), contrasting with the higher shifts observed upon direct substitution at the bpy ligand (on the order of 5–20 cm^{-1}),[23] and can be explained by the remote character of substitution in the complexes described herein.

Character of the Lowest Excited States. We now turn to (TD-)DFT calculations to understand the effects of the substituents in the electronic structures of these complexes. We observe an increase in the relative energies of the HOMOs and LUMOs with more donating groups, with the energies of the latter having a more pronounced dependence (Figure S4).

While the location of the LUMO remains largely unaltered throughout the series, we observe that, as the electron-donating character of the substituent is increased, the HOMO gradually shifts from the $\{Re(CO)_3\}^+$ moiety to the 4′-phenyl moiety of the terpy ligand (Figure 4), until it is localized entirely on the latter, for $R^1 = NMe_2$.

These observations are supported by the charge-density-difference (CDD) isosurfaces calculated for the $S_1 \leftarrow S_0$ transition, as shown in Figure 5 for the unsubstituted and OMe- and NMe_2-substituted complexes (**2d**–**2f**, respectively). The CDD isosurfaces were calculated using *MultiWfn*, version 3.5.[54]

For complex **2d** (and those with more electron-withdrawing substituents), it is clear that this transition has the expected MLCT character. Surprisingly, despite the change in the localization of the HOMO observed for complex **2e**, the $S_1 \leftarrow S_0$ transition conserves an MLCT character (further supported

https://dx.doi.org/10.1021/acs.inorgchem.0c01939
Inorg. Chem. XXXX, XXX, XXX–XXX

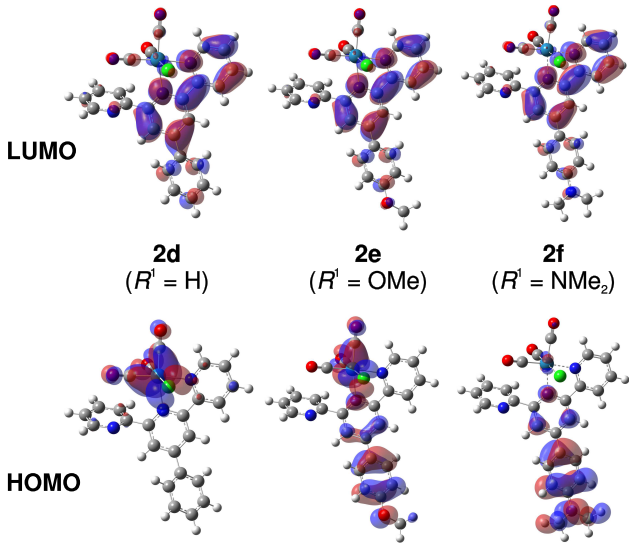

Figure 4. Calculated HOMOs and LUMOs of **2d**–**2f**. Orbitals shown at $|\phi| = 0.025$ au.

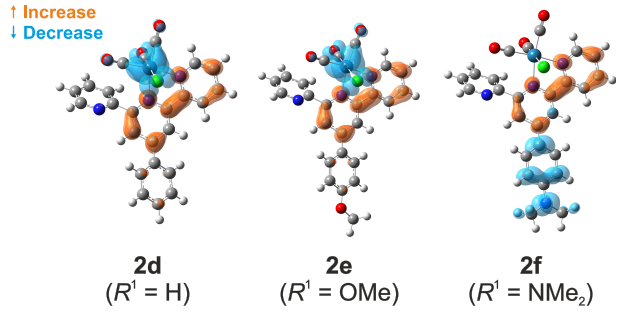

Figure 5. CDD isosurfaces of the $S_1 \leftarrow S_0$ transition of **2d**–**2f**, shown at $|\Delta\rho| = 0.002$ au.

by TRIR data and discussed next). In contrast, the $S_1 \leftarrow S_0$ transition in the NMe_2-substituted complex has strong ILCT character—with the NMe_2 group acting as the donor and the metal-coordinated κ^2N-terpy as the acceptor.

Excited-State Dynamics. To understand the excited-state dynamics of these complexes, we performed transient absorption experiments with UV pump and ultrashort broadband mid-IR pulses derived from a home-built optical parametric amplifier as the probe (complete experimental details are given in section 1.3 of the SI).[55−57]

TRIR spectra of complexes **2a**–**2e** in air-saturated DMF, recorded upon excitation with 420 nm ultrashort pulses, show the typical features of the ^{3}MLCT excited state of rhenium(I) tricarbonyl dyes within 500 fs of excitation. The TRIR spectra of **2d** as a representative example is shown in Figure 6. These bands show a time-dependent blue shift, on a time scale of ca. 5 ps, attributed to a convolution of ultrafast intersystem crossing (ISC; within ∼100 fs) and vibrational relaxation on the excited state, in agreement with previous reports.[10,48,58]

For complex **2f**, the situation is different: TRIR spectroscopy yielded definitive experimental evidence for a ^{3}ILCT state in this complex. Immediately after excitation, we observed in the TRIR spectra of **2f** in DMF (Figure 7) two sets of excited-state-absorption (ESA) bands in the ν_{CO} region: a single, clearly resolved band around 1994 cm^{-1} and a set of two unresolved bands in the 1860 cm^{-1} region that partially overlap with the ground-state bleaches.

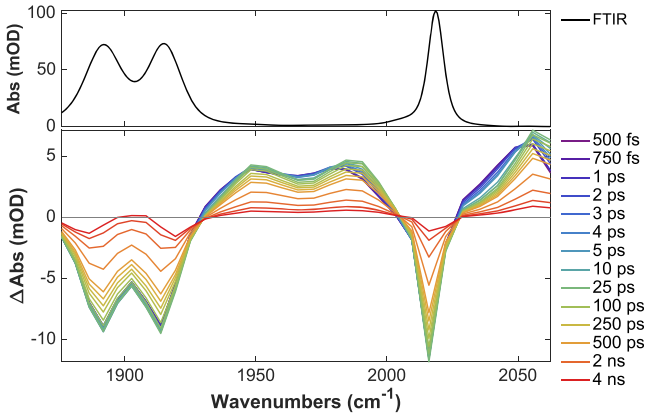

Figure 6. FT-IR spectrum (top) and magic-angle UV pump–IR probe transient spectra (bottom) of **2d** (5 mM in DMF) at different pump–probe delays.

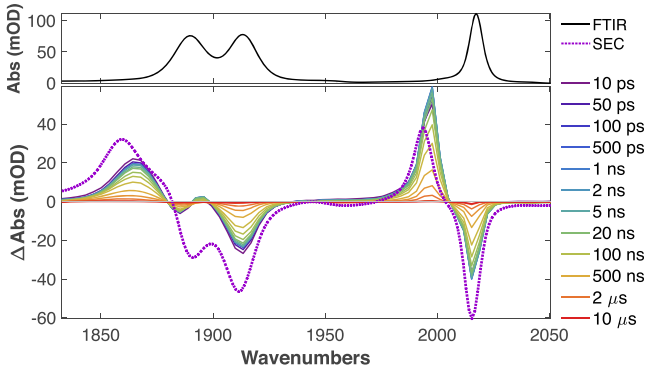

Figure 7. FT-IR spectrum (top) and UV pump–IR probe transient spectra (bottom) of **2f** (5 mM in nitrogen-purged DMF) at different delays (picosecond to microsecond time scales). The IR-SEC difference spectrum at −1.8 V versus Fc^+/Fc (first reduction) is overlaid with the pump–probe spectra (purple dotted line, ΔAbs × 0.4).

The red shifts of the ESA bands suggest an increase of the electron density around the rhenium(I) center upon photoexcitation, closely resembling the difference spectra of the singly reduced species (Figure 7, purple dotted line) observed by IR-SEC studies. These features are very well reproduced by DFT calculations of the lowest triplet excited state and the singly reduced NMe_2-substituted complex (Figure S5). After the initial blue shift of the bands in a 5 ps time scale, the observed signal remained constant for more than 4 ns (Figure S6). To observe the decay of these features (and, hence, extract the actual excited-state lifetimes), we performed a second set of TRIR measurements comprising time scales from 10 ps to over 10 μs, using a setup based on two synchronized amplifiers.[59] From these measurements, we obtained a lifetime of 380 ± 20 ns in a nitrogen-purged DMF solution for **2f**. The significantly longer lifetime of this complex (ca. 260 times longer than that of **2d**) can be explained by the different character of the lowest triplet excited states.

These observations contrast with the TRIR data of complexes **2a**–**2e** (Figure 6). In those cases, excitation of the MLCT band *decreases* the electron density around the metal center (as evidenced by blue-shifted ESA bands) and the transient signals decay significantly faster.

On the picosecond-to-microsecond setup and under the same measurement conditions, we obtained a lifetime of 2.3 ±

https://dx.doi.org/10.1021/acs.inorgchem.0c01939
Inorg. Chem. XXXX, XXX, XXX−XXX

0.2 ns for **2e** (R^1 = OMe) in nitrogen-purged DMF, which agrees quantitatively with the lifetime obtained in the ultrafast experiments in air-saturated DMF solutions. This illustrates the negligible effects of oxygen on the lifetimes of all other complexes, showing also the consistency of the kinetics obtained from the different setups.

The photophysical properties of the ILCT states of rhenium(I) tricarbonyls have been previously studied in complexes bearing 3-substituted 1-(2-pyridyl)imidazo[1,5-α]-pyridine ligands.[48] The ILCT character of these complexes was largely independent from the substituents (ranging from NO_2 to NMe_2), in sharp contrast with our observation for the rhenium(I) complexes with 4′-(4-R^1-phenyl)-2,2′:6′,2″-terpyridine ligands. In our case, only the NMe_2-substituted complex (**2f**) shows a significant ILCT, displaying similar characteristic TRIR signatures, but a significantly longer excited-state lifetime.

A complementary approach, based on tuning of the axial ligand, has also shown that ^{3}ILCT lifetimes can be modulated from 27 ns to 6 μs when the axial ligand is changed from pyridine to bromide. This opens additional pathways for future modifications of the complexes studied in this work and highlights the interplay between close-lying MLCT and long-lived ILCT states. In their work, Gordon and co-workers show that the change in the emission lifetimes does not arise from the switching of molecular orbitals (as in our case, where the HOMO shifts with the substituent), close-lying deactivating states, contributions from a halide-to-ligand charge-transfer state, or changes in spin−orbit coupling.[60]

In our case, we observe a systematic change in the ^{3}MLCT lifetimes and reduction potentials with different substituents on the terpy ligand (Figures 8 and S7). The lifetimes increase

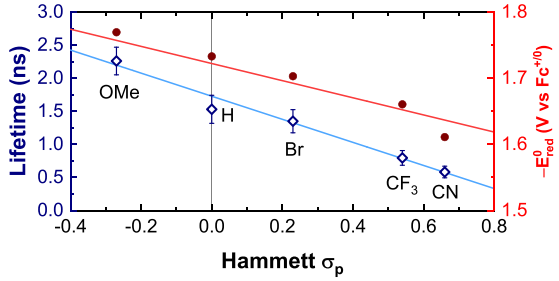

Figure 8. Linear correlations between the ^{3}MLCT lifetimes (from TRIR, in blue), the observed ground-state reduction potentials (in red), and the Hammett σ_p substituent constants for complexes **2a**−**2e**. Complex **2f** deviates significantly from the linearity of the lifetime plot and is excluded for clarity.

from 0.58 to 2.3 ns between the CN- and OMe-substituted complexes, while the reduction potentials become more negative, shifting from −1.6 to −1.8 V versus ferrocenium/ferrocene (Fc^+/Fc; discussed next). The fitted lifetimes of all complexes can be found in Table S2.

The frequency shift of −17 cm^{-1} observed for the a′(1) band in the TRIR spectra of **2f** in DMF is similar to the ca. −20 cm^{-1} shift reported for complexes with 3-substituted 1-(2-pyridyl)imidazo[1,5-α]pyridine ligands (possessing also an ILCT excited state)[48] and the ca. −24 cm^{-1} shift observed upon electron transfer from the porphyrin to the rhenium moiety in the porphyrin-appended rhenium(I) tricarbonyl complexes studied by Perutz and co-workers.[32] The latter, however, is in better agreement with the −24 cm^{-1} shift observed for the singly reduced **2f**$^-$, obtained by spectroelectrochemistry (see below). Overall, these numbers illustrate the small but significant difference between a *formally* reduced complex and an *apparent* reduced environment around the *fac*-$\{Re(CO)_3\}^+$ moiety arising from intramolecular charge transfer in the excited state.

Photochemical and Redox Properties. To better understand the excited-state properties and to estimate the applicability of these complexes as photosensitizers, we evaluated the excited-state redox potentials, which were estimated according to eqs 1 and 2:

$$E_{red}{}^{o\prime}(^3[Re^I]^*) = E_{red}{}^{o\prime} + \Delta G_{ST} \quad (1)$$

$$E_{ox}{}^{o\prime}(^3[Re^I]^*) = E_{ox}{}^{o\prime} - \Delta G_{ST} \quad (2)$$

where $E_{red}{}^{o\prime}$ and $E_{ox}{}^{o\prime}$ are the ground-state reduction and oxidation potentials, respectively, and ΔG_{ST} is the singlet−triplet energy gap.

The ground-state redox properties of these complexes were studied by cyclic voltammetry (CV) in 0.1 M $[Bu_4N][PF_6]$ in DMF at room temperature. The cyclic voltammograms of selected complexes are shown in Figure 9. All complexes show

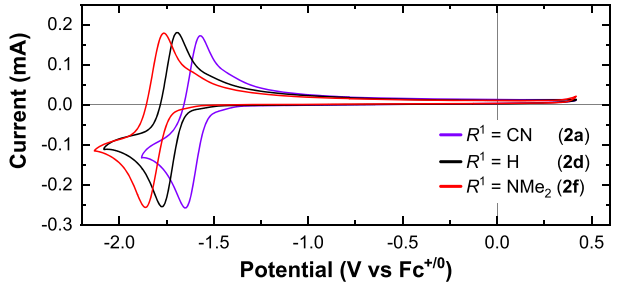

Figure 9. Cyclic voltammograms of selected complexes in 0.1 M $[Bu_4N][PF_6]$ in DMF. Scan rate: 100 mV s^{-1}.

a partially irreversible two-electron reduction ($E_{red}{}^{o\prime}$), taking place at ca. −1.7 V versus Fc^+/Fc. The oxidation was outside of the electrochemical window of our experiment ($E_{ox}{}^{o\prime}$ > 0.5 V vs Fc^+/Fc).

From this, we observe that $E_{red}{}^{o\prime}$ becomes more negative with more electron-donating substituents (Table 1), showing an excellent linear correlation with the Hammett σ_p substituent constants (Figure 8). This demonstrates that tunability in a range of ±200 mV can be achieved without significantly altering the optical properties of these complexes (for **2a**−**2e**),

Table 1. Ground- and Excited-State Redox Properties of the Studied Complexes in DMF

	R^1	$E_{red}{}^{o\prime}$ (V)[a]	ΔG_{ST}^{exp} (eV)[b]	ΔG_{ST}^{theo} (eV)[c]	$(E_{red}{}^{o\prime})^*$ (V)[d]
2a	CN	−1.61	2.42	2.38	0.80
2b	CF_3	−1.66	2.46	2.44	0.79
2c	Br	−1.70	2.46	2.46	0.76
2d	H	−1.73	2.48	2.49	0.75
2e	OMe	−1.77	2.50	2.47	0.73
2f	NMe_2	−1.81	2.37	2.06	0.56

[a]Electrochemical potential in volts versus Fc^+/Fc in DMF. [b]From a linear fit of the high-energy side of the 77 K emission spectrum in 2-MeTHF. [c]Energy difference between the optimized ground-state and lowest triplet excited-state structures. [d]Excited-state potentials calculated from eq 1.

https://dx.doi.org/10.1021/acs.inorgchem.0c01939
Inorg. Chem. XXXX, XXX, XXX−XXX

a desirable feature for fine-tuning of the energetics of ground- and excited-state electron-transfer processes involving these complexes.

At the same time, we note that the long-lived ILCT state achieved in the NMe_2-substituted complex still has comparable excited-state reduction potentials (only ca. 200 mV below those of the rest of the complexes in the series), while absorbing light with comparable extinction coefficients over 100 nm further to the red.

The emission spectra of all complexes were measured in DMF at room temperature and at 77 K in a 2-methyltetrahydrofuran (2-MeTHF) glass (Figure S8). The ΔG_{ST} values were obtained from a linear fit of the high-energy side of the low-temperature emission spectra, as described previously (Figure S9).[22] These values also show a very good correlation with the Hammett σ_p substituent constants (except for **2f**) and illustrate that more electron-donating substituents can increase ΔG_{ST} up to a certain limit, before any further increase in the electron density results in a *decrease* of ΔG_{ST} instead.

At room temperature, all complexes exhibit a moderately intense, broad, and unstructured emission (very strong in the case of the NMe_2 complex, **2f**). The positions of the emission maxima correlate well with the Hammett σ_p substituent constants, showing a blue shift with more electron-donating groups. At cryogenic temperatures (77 K), the emission spectra of complexes **2a**−**2e** show significant hypsochromic shifts, characteristic of emission from a ^{3}MLCT state. Complex **2f**, in contrast, deviates significantly from this behavior. The emission of **2f** shows instead a bathochromic shift upon cooling and the appearance of a vibronic structure, suggestive of emission from a ligand-localized triplet state.[61] These observations suggest that the character of the lowest triplet excited state of the NMe_2-substituted complex changes upon cooling. At room temperature, it has significant ILCT character, also supported by the results discussed in the previous section.

The DFT-calculated ΔG_{ST} values for the κ^2N complexes were in excellent agreement with those found in the experiment, with a mean deviation of ±0.02 eV for all complexes (except **2f**, which deviated by −0.3 eV). The ground- and excited-state redox properties are summarized in Table 1.

To identify the spectral signatures of the redox species observed in the CV experiments, we performed IR-SEC studies in 0.1 M $[Bu_4N][PF_6]$ in DMF. The IR-SEC spectra of **2d** are shown in Figure 10 as a representative example.

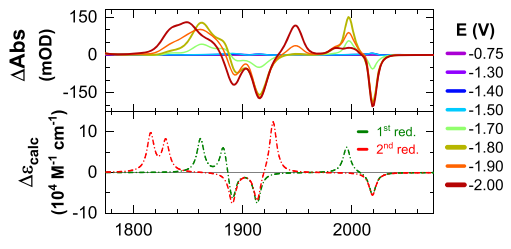

Figure 10. Experimental (solid lines) and calculated (dashed lines) difference IR spectra of the redox states of **2d**. Experimental spectra measured in 0.1 M $[Bu_4N][PF_6]$ in DMF. Potentials versus Fc^+/Fc. Theoretical frequencies were scaled by 0.97 to better match the experimentally obtained values.

The two-electron reduction process could be resolved in the IR-SEC experiments into two overlapping and consecutive single-electron reductions, as evidenced by significant incremental red shifts of the ν_{CO} bands (Figure 10).

Further evidence for the two-electron nature of this reduction comes from the ca. 96 mV peak-to-peak separation (at a scan rate of 100 mV s^{-1}) and the small shoulder observed at less negative potentials (Figure 9). In all cases, an excellent agreement was found between the calculated and experimental difference spectra of the corresponding redox states. The partial irreversibility of the second reduction process is attributed in both cases to the loss of chloride ligands (also reproduced in the DFT calculations, where optimization of the doubly reduced species led to chlorine dissociation), agreeing with previous reports of related complexes.[62]

Photocatalytic Hydrogen Evolution Experiments. Considering the excited-state redox potentials and lifetimes exhibited by these complexes, we performed a series of homogeneous proof-of-principle photocatalysis experiments in DMF. To focus only on the hydrogen evolution half-reaction, triethanolamine (TEOA, 1 M) was used as a sacrificial electron donor and triflic acid (TfOH, 0.1 M) as the proton source. For these test experiments, we chose $[Co(dmgH)_2]^{2+}$ (0.5 mM) as a catalyst, which was prepared in situ from $Co(BF_4)_2{\cdot}6H_2O$ and excess dimethylglyoxime ($dmgH_2$). As representative examples, we tested complexes **2d** and **2f**, as well as $[Re(bpy)(CO)_3(NCS)]$ (**RePS**) under the same conditions (with [Re] = 0.5 mM and λ_{exc} = 390 nm). The latter complex was used to benchmark the performance of our complexes in comparison to a well-studied system.[63,64]

Under these conditions, we observed significant and prolonged hydrogen evolution only for **2d** (Figure S10), yielding a final turnover number (TON) for the photosensitizer of 580 ± 40 over 7 days. We observed a bimodal decay of the turnover frequency (TOF) and a significant decrease in the rate after 4.5 days. These results suggest that the integrity of the catalyst represents the limiting factor for the long-term stability of this photocatalytic system, as discussed in previous reports of related systems.[65] We did not observe hydrogen evolution using complex **2f** at these high concentrations, which we attribute to accumulation of the reduced photosensitizer and subsequent degradation.[64]

Considering this last result and the very long lifetime of complex **2f** and its intense absorption extending until ca. 500 nm, we performed additional photocatalytic experiments (Figure 11) with λ_{exc} = 453 nm and higher $dmgH_2$ concentrations (3.5 mM), while using a 10-fold lower photosensitizer concentration ([**2f**] = 50 μM). All other parameters were kept constant.

The very high TONs (2130 ± 120) and hydrogen production rates (up to ca. 40 nmol s^{-1}) obtained under these conditions compare very favorably with those obtained for a closely related system using **RePS** as the photosensitizer.[63,64] While strict comparisons of the TOF and TON values are inadequate, it is worth mentioning that, under these conditions, complex **2f** is a remarkably stable photosensitizer. The results shown in this work constitute, to the best of our knowledge, the first example of a system, where the long-lived ^{3}ILCT state of a rhenium(I) complex is used for photocatalytic hydrogen production, being involved in multielectron transfer steps in an efficient manner. We believe that the long-term stability of this system might be improved by

https://dx.doi.org/10.1021/acs.inorgchem.0c01939
Inorg. Chem. XXXX, XXX, XXX−XXX

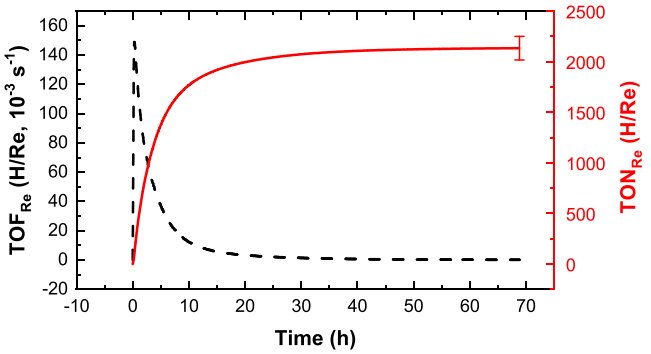

Figure 11. Hydrogen evolution from **2f** as a photosensitizer. Conditions: [**2f**] = 50 μM, [Co] = 0.5 mM, [dmgH$_2$] = 3.5 mM, 1 M TEOA, 0.1 M TfOH in DMF, and λ_{exc} = 453 nm.

fine-tuning of the conditions of the photocatalytic experiments, which are outside the scope of the present work.

To gain a deeper understanding of the initial photochemical steps in the photocatalytic cycle and, in particular, to evaluate the potential differences between the ILCT and MLCT excited-state reactivities, we performed emission quenching, as well as TRIR experiments in the picosecond-to-microsecond time scales of complexes **2d** and **2f** in the presence of TEOA. For **2d**, we observed a very small change in the excited-state kinetics and emission intensities, leading to a diffusion-limited quenching rate $k_Q \approx 4 \times 10^8$ M^{-1} s^{-1}. We find this number of qualitative character, given the very short lifetime of **2d**, which limits the possibility of studying the intermolecular electron-transfer steps in this complex.

Complex **2f**, in contrast, presented an unexpected behavior. Upon the addition of TEOA, we observed the appearance of a strongly emissive blue-shifted band whose intensity increased with increasing concentrations of TEOA. The absorption spectra remained unchanged. At the same time, the spectral features and kinetics of **2f** (1 mM in degassed DMF) remained largely unchanged in a concentration range from 1 mM to 1 M TEOA (containing 10 mol % TfOH), hinting at a different order of events in the photocatalytic cycle of **2f**. TRIR spectra recorded in the absence of TfOH also did not show any difference with respect to those of pure **2f** in DMF.

In the "conventional" photocycle, the ^{3}MLCT excited state of a rhenium(I) complex (like **RePS**) is reductively quenched in a bimolecular fashion by TEOA, and it is this reduced species that transfers the electrons to the proton reduction catalyst.[14,64] If the ^{3}ILCT excited state of **2f** is not quenched by TEOA—and given the fact that the system *does* evolve significant amounts of hydrogen—we hypothesize that this complex transfers the electron directly to the cobalt catalyst (considering its very long lifetime). After this electron transfer, the oxidized **2f**$^+$ is regenerated by TEOA at longer time scales.

To prove this hypothesis, we performed TRIR experiments of **2f** with different concentrations of [Co(dmgH)$_2$]$^{2+}$ ranging from 10 to 75 mM (the cobalt complex was prepared as a stock solution from anhydrous $CoBr_2$ and 3 equiv of dmgH$_2$ in DMF). From Stern–Volmer analysis of the TRIR kinetic data (Figure S11), we obtained a second-order quenching rate constant of k_{Co} = (2.0 ± 0.2) × 10^8 M^{-1} s^{-1} for electron transfer between **2f** and [Co(dmgH)$_2$]$^{2+}$. This value of k_{Co} compares very well with the reported values of 1.3 × 10^8 and 2.5 × 10^8 M^{-1} s^{-1} for electron transfer between reduced **RePS**$^-$ or [Re(bpy)(CO)$_3$Br]$^-$, respectively, and [Co(dmgH)$_2$]$^{2+}$. This rate is also significantly slower than the 1.23 × 10^9 M^{-1} s^{-1} quenching rate between photoexcited **RePS*** and [Co(dmgH)$_2$]$^{2+}$, thus excluding this mechanism.[64]

The absence of new transient features and long-lived signals in the TRIR spectra of **2f** with [Co(dmgH)$_2$]$^{2+}$ (independent of the presence of TEOA) may suggest that either (i) a fast back electron transfer from the cobalt complex in the absence of TEOA or (ii) a fast electron transfer from TEOA (present in large excess) to **2f**$^+$ takes place after the initial quenching event in the three-component system.

Combining the insights gained from these experiments, we believe that the formation of an exciplex between excited **2f*** and TEOA can simultaneously explain the changes in the emission spectra and the unchanged TRIR data. The formation of a metal complex–molecule exciplex has been observed before,[66] with the case of [Re(4,7-diphenyl-1,10-phenanthroline)(CO)$_3$Cl] and *N*,*N*-dimethylaniline (DMA) in decalin being particularly relevant in the context of our work. In this system, even very low concentrations (~10^{-3} M) of DMA were enough to observe a new red-shifted emission band.[67] While our specific scenario is different—namely, a more polar solvent and a different quencher—complex **2f** has very large charge-transfer character upon photoexcitation (as shown in Figure 5), leading to a large change in the dipole moment, which would render the formation of a charge-transfer exciplex with TEOA feasible.

Additional mechanistic studies of these complexes with the purpose of unravelling the nature of this process and its solvent dependence will reveal further differences in the reactivity and photophysical properties of the ^{3}ILCT versus ^{3}MLCT excited states, easily switched in these complexes by remote substitution in the ligand framework.

CONCLUDING REMARKS

The ground and excited states of a series of rhenium(I) tricarbonyl complexes with substituted 4′-(4-R^1-phenyl)-2,2′:6′,2″-terpyridine ligands were analyzed by steady-state and time-resolved spectroscopic methods. We found excellent correlations between the evaluated spectroscopic and electrochemical properties of these complexes and the Hammett σ_p substituent constants, showing their tunability even by changing the substituent in a remote position of the ligand framework. CV and IR-SEC revealed an irreversible stepwise two-electron reduction, which, in turn, allowed us to assign the identities and spectral signatures of the one- and two-electron-reduced species.

The NMe$_2$-substituted complex (**2f**) showed notably exceptional lifetime and spectroscopic properties compared to other complexes of the same series. In this complex, the lowest singlet and triplet excited states both have ILCT character, as demonstrated by TRIR and emission spectra, and are supported by detailed (TD-)DFT calculations. The particularly long triplet lifetime of ca. 380 ns obtained for the NMe$_2$-substituted complex (vs ca. 1.5 ns for the unsubstituted complex) suggests that very strongly donating groups can lead to distinct photophysical and photochemical properties and opens new avenues to exploring further substituent-related modifications to the terpyridine ligand framework. We conclude that judicious ligand-based substitutions can still be exploited to access long-lived, strongly emissive yet sufficiently reducing excited states of complexes with significantly red-shifted absorption, which would perform as better photosensitizers by using a wider portion of the solar

https://dx.doi.org/10.1021/acs.inorgchem.0c01939
Inorg. Chem. XXXX, XXX, XXX–XXX

spectrum. In this regard, our approach to enhancing light absorption through remote substitution is complementary to those that have been explored so far and benefits from the simplicity and scalability of the synthesis of the substituted terpyridine ligands.

In proof-of-principle homogeneous photocatalytic experiments, we demonstrated stable hydrogen evolution over a period of 7 days with complex **2d** and a fast and sustained hydrogen evolution from complex **2f** in a photocatalytic system with 10-fold-smaller photosensitizer concentrations, reaching TONs of over 2100 using standard $[Co(dmgH)_2]^{2+}$ as a catalyst. Using TRIR spectroscopy, we tentatively assign direct electron transfer from **2f*** to the proton reduction catalyst, instead of reductive quenching by the sacrificial donor (TEOA). Further mechanistic studies are needed to explain this in detail, focusing on the differences in the reactivity between complexes operating from a ^{3}ILCT versus ^{3}MLCT excited state. The application of **2f** for photocatalytic hydrogen evolution constitutes, to the best of our knowledge, the first example of the use of long-lived ^{3}ILCT states in rhenium(I) tricarbonyl complexes for photocatalytic hydrogen production and shows the potential of the terpyridine framework for further modifications and mechanistic studies of the rich photochemistry of these complexes.

■ ASSOCIATED CONTENT

Supporting Information

The Supporting Information is available free of charge at https://pubs.acs.org/doi/10.1021/acs.inorgchem.0c01939.

Full experimental details (including synthetic procedures, characterization details, crystallographic discussions, details about the transient absorption and electrochemistry experiments), UV−vis absorption, emission, NMR and FT-IR spectra of all complexes, IR spectroelectrochemical data, details of the computational calculations, and additional tables and figures (PDF)

Accession Codes

CCDC 2012296−2012298 contain the supplementary crystallographic data for this paper. These data can be obtained free of charge via www.ccdc.cam.ac.uk/data_request/cif, or by emailing data_request@ccdc.cam.ac.uk, or by contacting The Cambridge Crystallographic Data Centre, 12 Union Road, Cambridge CB2 1EZ, UK; fax: +44 1223 336033.

■ AUTHOR INFORMATION

Corresponding Author

Ricardo Fernández-Terán − *Department of Chemistry, University of Zurich, Zurich CH-8006, Switzerland;* orcid.org/0000-0002-4665-3520; Phone: +41 44 635 44 73; Email: Ricardo.Fernandez@chem.uzh.ch; Fax: +41 44 635 68 38

Author

Laurent Sévery − *Department of Chemistry, University of Zurich, Zurich CH-8006, Switzerland;* orcid.org/0000-0002-6546-379X

Complete contact information is available at: https://pubs.acs.org/10.1021/acs.inorgchem.0c01939

Funding

This research was funded through the Swiss National Science Foundation (Sinergia Project CRSII2 160801/1 and AP Energy Grant PYAPP2 160586) and the University Research Priority Program for Solar Light into Chemical Energy Conversion (LightChEC) of the University of Zurich.

Notes

The authors declare no competing financial interest.

■ ACKNOWLEDGMENTS

We thank Prof. Dr. Peter Hamm and Prof. Dr. S. David Tilley for their valuable input and encouragement. We thank Prof. Dr. Roger Alberto and his group for allowing us to use the photochemical hydrogen evolution detection system and laboratory infrastructure. Dr. Benjamin Probst-Rüd is gratefully acknowledged for his valuable support in the photocatalytic hydrogen evolution experiments and insightful discussions. Prof. Dr. Bernhard Spingler is acknowledged for helpful crystallographic discussions. We also thank Dr. Jan Helbing and Gökçen Tek for insightful discussions and Olga Božović for proofreading the manuscript and providing helpful comments.

■ REFERENCES

(1) Takeda, H.; Koike, K.; Inoue, H.; Ishitani, O. Development of an efficient photocatalytic system for CO_2 reduction using rhenium(I) complexes based on mechanistic studies. *J. Am. Chem. Soc.* **2008**, *130*, 2023.

(2) Takeda, H.; Ishitani, O. Development of efficient photocatalytic systems for CO_2 reduction using mononuclear and multinuclear metal complexes based on mechanistic studies. *Coord. Chem. Rev.* **2010**, *254*, 346.

(3) Kumar, B.; Llorente, M.; Froehlich, J.; Dang, T.; Sathrum, A.; Kubiak, C. P. Photochemical and Photoelectrochemical Reduction of CO_2. *Annu. Rev. Phys. Chem.* **2012**, *63*, 541.

(4) Morimoto, T.; Nakajima, T.; Sawa, S.; Nakanishi, R.; Imori, D.; Ishitani, O. CO_2 capture by a rhenium(I) complex with the aid of triethanolamine. *J. Am. Chem. Soc.* **2013**, *135*, 16825.

(5) Kou, Y.; Nabetani, Y.; Masui, D.; Shimada, T.; Takagi, S.; Tachibana, H.; Inoue, H. Direct detection of key reaction intermediates in photochemical CO_2 reduction sensitized by a rhenium bipyridine complex. *J. Am. Chem. Soc.* **2014**, *136*, 6021.

(6) Schreier, M.; Gao, P.; Mayer, M. T.; Luo, J.; Moehl, T.; Nazeeruddin, M. K.; Tilley, S. D.; Grätzel, M. Efficient and selective carbon dioxide reduction on low cost protected Cu_2O photocathodes using a molecular catalyst. *Energy Environ. Sci.* **2015**, *8*, 855.

(7) Yi, X.; Zhao, J.; Sun, J.; Guo, S.; Zhang, H. Visible light-absorbing rhenium(I) tricarbonyl complexes as triplet photosensitizers in photooxidation and triplet−triplet annihilation upconversion. *J. Chem. Soc. Dalt. Trans.* **2013**, *42*, 2062.

(8) Patrocinio, A. O. T.; Frin, K. P.; Murakami Iha, N. Y. Solid state molecular device based on a rhenium(I) polypyridyl complex immobilized on TiO_2 films. *Inorg. Chem.* **2013**, *52*, 5889.

(9) Gao, Y.; Sun, S.; Han, K. Electronic structures and spectroscopic properties of rhenium (I) tricarbonyl photosensitizer: $[Re(4,4'-(COOEt)_2-2,2'-bpy)(CO)_3py]PF_6$. *Spectrochim. Acta, Part A* **2009**, *71*, 2016.

(10) el Nahhas, A.; Consani, C.; Blanco-Rodríguez, A. M.; Lancaster, K. M.; Braem, O.; Cannizzo, A.; Towrie, M.; Clark, I. P.; Záliš, S.; Chergui, M.; Vlček, A. Ultrafast excited-state dynamics of rhenium(I) photosensitizers $[Re(Cl)(CO)_3(N,N)]$ and $[Re(imidazole)-(CO)_3(N,N)]^+$: Diimine effects. *Inorg. Chem.* **2011**, *50*, 2932.

(11) Anfuso, C. L.; Snoeberger, R. C.; Ricks, A. M.; Liu, W.; Xiao, D.; Batista, V. S.; Lian, T. Covalent attachment of a rhenium bipyridyl CO_2 reduction catalyst to rutile TiO_2. *J. Am. Chem. Soc.* **2011**, *133*, 6922.

(12) Liu, J.; Jiang, W. Photoinduced hydrogen evolution in supramolecular devices with a rhenium photosensitizer linked to FeFe-hydrogenase model complexes. *Dalt. Trans.* **2012**, *41*, 9700.

(13) Abdellah, M.; El-Zohry, A. M.; Antila, L. J.; Windle, C. D.; Reisner, E.; Hammarström, L. Time-resolved IR spectroscopy reveals a mechanism with TiO_2 as a reversible electron acceptor in a TiO_2–Re catalyst system for CO_2 photoreduction. *J. Am. Chem. Soc.* **2017**, *139*, 1226.
(14) Probst, B.; Guttentag, M.; Rodenberg, A.; Hamm, P.; Alberto, R. Photocatalytic H_2 production from water with rhenium and cobalt complexes. *Inorg. Chem.* **2011**, *50*, 3404.
(15) Guttentag, M.; Rodenberg, A.; Kopelent, R.; Probst, B.; Buchwalder, C.; Brandstätter, M.; Hamm, P.; Alberto, R. Photocatalytic H2 production with a rhenium/cobalt system in water under acidic conditions. *Eur. J. Inorg. Chem.* **2012**, *2012*, 59.
(16) Guttentag, M.; Rodenberg, A.; Bachmann, C.; Senn, A.; Hamm, P.; Alberto, R. A highly stable polypyridyl-based cobalt catalyst for homo- and heterogeneous photocatalytic water reduction. *Dalt. Trans.* **2013**, *42*, 334.
(17) Rodenberg, A.; Orazietti, M.; Probst, B.; Bachmann, C.; Alberto, R.; Baldridge, K. K.; Hamm, P. Mechanism of photocatalytic hydrogen generation by a polypyridyl-based cobalt catalyst in aqueous solution. *Inorg. Chem.* **2015**, *54*, 646.
(18) Rodenberg, A.; Orazietti, M.; Mosberger, M.; Bachmann, C.; Probst, B.; Alberto, R.; Hamm, P. Quinones as Reversible Electron Relays in Artificial Photosynthesis. *ChemPhysChem* **2016**, *17*, 1321.
(19) Kalyanasundaram, K. Photophysics, photochemistry and solar energy conversion with tris(bipyridyl)ruthenium(II) and its analogues. *Coord. Chem. Rev.* **1982**, *46*, 159.
(20) Juris, A.; Campagna, S.; Bidd, I.; Lehn, J. M.; Ziessel, R. Synthesis and photophysical and electrochemical properties of new halotricarbonyl(polypyridine)rhenium(I) complexes. *Inorg. Chem.* **1988**, *27*, 4007.
(21) Wrighton, M.; Morse, D. L. The Nature of the Lowest Excited State in Tricarbonylchloro-1,10-phenanthrolinerhenium(I) and Related Complexes. *J. Am. Chem. Soc.* **1974**, *96*, 998.
(22) Kurtz, D. A.; Brereton, K. R.; Ruoff, K. P.; Tang, H. M.; Felton, G. A.; Miller, A. J.; Dempsey, J. L. Bathochromic Shifts in Rhenium Carbonyl Dyes Induced through Destabilization of Occupied Orbitals. *Inorg. Chem.* **2018**, *57*, 5389.
(23) Worl, L. A.; Duesing, R.; Chen, P.; Ciana, L. D.; Meyer, T. J. Photophysical properties of polypyridyl carbonyl complexes of rhenium(I). *J. Chem. Soc., Dalton Trans.* **1991**, 849.
(24) Ley, K.; Schanze, K. Photophysics of metal-organic π-conjugated polymers. *Coord. Chem. Rev.* **1998**, *171*, 287.
(25) Zarkadoulas, A.; Koutsouri, E.; Kefalidi, C.; Mitsopoulou, C. A. Rhenium complexes in homogeneous hydrogen evolution. *Coord. Chem. Rev.* **2015**, *304–305*, 55.
(26) Portenkirchner, E.; Schlager, S.; Apaydin, D.; Oppelt, K.; Himmelsbach, M.; Egbe, D. A.; Neugebauer, H.; Knör, G.; Yoshida, T.; Sariciftci, N. S. Using the Alkynyl-Substituted Rhenium(I) Complex (4,4′-Bisphenyl-Ethynyl-2,2′-Bipyridyl)$Re(CO)_3Cl$ as Catalyst for CO_2 Reduction—Synthesis, Characterization, and Application. *Electrocatalysis* **2015**, *6*, 185.
(27) MacQueen, D. B.; Schanze, K. S. Free Energy and Solvent Dependence of Intramolecular Electron Transfer in Donor-Substituted Re(I) Complexes. *J. Am. Chem. Soc.* **1991**, *113*, 7470.
(28) MacQueen, D. B.; Schanze, K. S. Cation-Controlled Photophysics in a Re(I) Fluoroionophore. *J. Am. Chem. Soc.* **1991**, *113*, 6108.
(29) Stoeffler, H. D.; Thornton, N. B.; Temkin, S. L.; Schanze, K. S. Unusual Photophysics of a Rhenium(I) Dipyridophenazine Complex in Homogenous Solution and Bound to DNA. *J. Am. Chem. Soc.* **1995**, *117*, 7119.
(30) Lewis, J. D.; Perutz, R. N.; Moore, J. N. Proton-controlled photoisomerization: Rhenium(I) tricarbonyl bipyridine linked to amine or azacrown ether groups by a styryl pyridine bridging ligand. *Chem. Commun.* **2000**, *0*, 1865.
(31) Lewis, J. D.; Bussotti, L.; Foggi, P.; Perutz, R. N.; Moore, J. N. Picosecond forward electron transfer and nanosecond back electron transfer in an azacrown-substituted $[(bpy)Re(CO)_3(L)]^+$ complex: Direct observation by time-resolved UV-visible absorption spectroscopy. *J. Phys. Chem. A* **2002**, *106*, 12202.
(32) Gabrielsson, A.; Hartl, F.; Zhang, H.; Lindsay Smith, J. R.; Towrie, M.; Vlček, A.; Perutz, R. N. Ultrafast charge separation in a photoreactive rhenium-appended porphyrin assembly monitored by picosecond transient infrared spectroscopy. *J. Am. Chem. Soc.* **2006**, *128*, 4253.
(33) Kiyosawa, K.; Shiraishi, N.; Shimada, T.; Masui, D.; Tachibana, H.; Takagi, S.; Ishitani, O.; Tryk, D. A.; Inoue, H. Electron transfer from the porphyrin S2 state in a zinc porphyrin-rhenium bipyridyl dyad having carbon dioxide reduction activity. *J. Phys. Chem. C* **2009**, *113*, 11667.
(34) Gabrielsson, A.; Hartl, F.; Lindsay Smith, J. R.; Perutz, R. N. Photo-induced ligand substitution at a remote site via electron transfer in a porphyrin-appended rhenium carbonyl supermolecule. *Chem. Commun.* **2002**, *2*, 950.
(35) Kou, Y.; Nakatani, S.; Sunagawa, G.; Tachikawa, Y.; Masui, D.; Shimada, T.; Takagi, S.; Tryk, D. A.; Nabetani, Y.; Tachibana, H.; Inoue, H. Visible light-induced reduction of carbon dioxide sensitized by a porphyrin-rhenium dyad metal complex on p-type semiconducting NiO as the reduction terminal end of an artificial photosynthetic system. *J. Catal.* **2014**, *310*, 57.
(36) Mutai, T.; Cheon, J. D.; Arita, S.; Araki, K. Phenyl-substituted 2,2′:6′,2″-terpyridine as a new series of fluorescent compounds - Their photophysical properties and fluorescence tuning. *J. Chem. Soc. Perkin Trans. 2* **2001**, 1045.
(37) Fang, Y. Q.; Taylor, N. J.; Laverdière, F.; Hanan, G. S.; Loiseau, F.; Nastasi, F.; Campagna, S.; Nierengarten, H.; Leize-Wagner, E.; Van Dorsselaer, A. Ruthenium(II) complexes with improved photophysical properties based on planar 4′-(2-pyrimidinyl)-2,2′:6′,2″-terpyridine ligands. *Inorg. Chem.* **2007**, *46*, 2854.
(38) Hutchison, K.; Morris, J. C.; Nile, T. A.; Walsh, J. L.; Thompson, D. W.; Petersen, J. D.; Schoonover, J. R. Spectroscopic and photophysical properties of complexes of 4′-ferrocenyl-2,2′:6′,2″-terpyridine and related ligands. *Inorg. Chem.* **1999**, *38*, 2516.
(39) Crites, D. K.; Cunningham, C. T.; McMillin, D. R. Remarkable substituent effects on the photophysics of $Pt(4'\text{-X-trpy})Cl^+$ systems (trpy = 2,2′:6′,2″-terpyridine). *Inorg. Chim. Acta* **1998**, *273*, 346.
(40) Kong, C.; Peng, M.; Shen, H.; Wang, Y.; Zhang, Q.; Wang, H.; Zhang, J.; Zhou, H.; Yang, J.; Wu, J.; Tian, Y. A novel D-A type terpyridine-based carbazole Zn(II) complex with enhanced two-photon absorption and its bioimaging application. *Dyes Pigm.* **2015**, *120*, 328.
(41) Kam-Wing Lo, K.; Chung, C. K.; Chun-Ming Ng, D.; Zhu, N. Syntheses, characterisation and photophysical studies of novel biological labelling reagents derived from luminescent iridium(III) terpyridine complexes. *New J. Chem.* **2002**, *26*, 81.
(42) Wang, M.; Weyhermüller, T.; Bill, E.; Ye, S.; Wieghardt, K. Structural and Spectroscopic Characterization of Rhenium Complexes Containing Neutral, Monoanionic, and Dianionic Ligands of 2,2′-Bipyridines and 2,2′:6,2-Terpyridines: An Experimental and Density Functional Theory (DFT)-Computational Study. *Inorg. Chem.* **2016**, *55*, 5019.
(43) Laramée-Milette, B.; Zaccheroni, N.; Palomba, F.; Hanan, G. S. Visible and Near-IR Emissions from κ^2N- and κ^3N-Terpyridine Rhenium(I) Assemblies Obtained by an [n × 1] Head-to-Tail Bonding Strategy. *Chem. - Eur. J.* **2017**, *23*, 6370.
(44) Abel, E. W.; Dimitrov, V. S.; Long, N. J.; Orrell, K. G.; Osborne, A. G.; Pain, H. M.; Šik, V.; Hursthouse, M. B.; Mazid, M. A. 2,2′:6′,2″-Terpyridine (terpy) acting as a fluxional bidentate ligand. Part 2. Rhenium carbonyl halide complexes, *fac*-$[ReX(CO)_3(terpy)]$ (X = Cl, Br or I): NMR studies of their solution dynamics, synthesis of *cis*-$[ReBr(CO)_2(terp.$ *J. Chem. Soc., Dalton Trans.* **1993**, 597.
(45) Klemens, T.; Switlicka-Olszewska, A.; Machura, B.; Grucela, M.; Janeczek, H.; Schab-Balcerzak, E.; Szlapa, A.; Kula, S.; Krompiec, S.; Smolarek, K.; Kowalska, D.; Mackowski, S.; Erfurt, K.; Lodowski, P. Synthesis, photophysical properties and application in organic light emitting devices of rhenium(i) carbonyls incorporating functionalized 2,2′:6′,2″-terpyridines. *RSC Adv.* **2016**, *6*, 56335.

https://dx.doi.org/10.1021/acs.inorgchem.0c01939
Inorg. Chem. XXXX, XXX, XXX–XXX

(46) Klemens, T.; Switlicka-Olszewska, A.; Machura, B.; Grucela, M.; Schab-Balcerzak, E.; Smolarek, K.; Mackowski, S.; Szlapa, A.; Kula, S.; Krompiec, S.; Lodowski, P.; Chrobok, A. Rhenium(i) terpyridine complexes-synthesis, photophysical properties and application in organic light emitting devices. *Dalt. Trans.* **2016**, *45*, 1746.
(47) Klemens, T.; Czerwińska, K.; Szlapa-Kula, A.; Kula, S.; Świtlicka, A.; Kotowicz, S.; Siwy, M.; Bednarczyk, K.; Krompiec, S.; Smolarek, K.; Maćkowski, S.; Danikiewicz, W.; Schab-Balcerzak, E.; Machura, B. Synthesis, spectroscopic, electrochemical and computational studies of rhenium(i) tricarbonyl complexes based on bidentate-coordinated 2,6-di(thiazol-2-yl)pyridine derivatives. *Dalt. Trans.* **2017**, *46*, 9605.
(48) Blanco-Rodríguez, A. M.; Kvapilová, H.; Sýkora, J.; Towrie, M.; Nervi, C.; Volpi, G.; Záliš, S.; Vlček, A. Photophysics of Singlet and Triplet Intraligand Excited States in $[ReCl(CO)_3(1-(2-pyridyl)-imidazo[1,5-\alpha]pyridine)]$ Complexes. *J. Am. Chem. Soc.* **2014**, *136*, 5963.
(49) Shillito, G. E.; Preston, D.; Traber, P.; Steinmetzer, J.; McAdam, C. J.; Crowley, J. D.; Wagner, P.; Kupfer, S.; Gordon, K. C. Excited-State Switching Frustrates the Tuning of Properties in Triphenylamine-Donor-Ligand Rhenium(I) and Platinum(II) Complexes. *Inorg. Chem.* **2020**, *59*, 6736.
(50) Tu, S.; Jia, R.; Jiang, B.; Zhang, J.; Zhang, Y.; Yao, C.; Ji, S. Kröhnke reaction in aqueous media: one-pot clean synthesis of 4′-aryl-2,2′:6′,2″-terpyridines. *Tetrahedron* **2007**, *63*, 381.
(51) Sévery, L.; Siol, S.; Tilley, S. Design of Molecular Water Oxidation Catalysts Stabilized by Ultrathin Inorganic Overlayers—Is Active Site Protection Necessary? *Inorganics* **2018**, *6*, 105.
(52) Frisch, M. J.; Trucks, G. W.; Schlegel, H. B.; Scuseria, G. E.; Robb, M. A.; Cheeseman, J. R.; Scalmani, G.; Barone, V.; Mennucci, B.; Petersson, G. A.; Nakatsuji, H.; Caricato, M.; Li, X.; Hratchian, H. P.; Izmaylov, A. F.; Bloino, J.; Zheng, G.; Sonnenberg, J. L.; Hada, M.; Ehara, M.; Toyota, K.; Fukuda, R.; Hasegawa, J.; Ishida, M.; Nakajima, T.; Honda, Y.; Kitao, O.; Nakai, H.; Vreven, T.; Montgomery, J. A., Jr.; Peralta, J. E.; Ogliaro, F.; Bearpark, M.; Heyd, J. J.; Brothers, E.; Kudin, K. N.; Staroverov, V. N.; Kobayashi, R.; Normand, J.; Raghavachari, K.; Rendell, A.; Burant, J. C.; Iyengar, S. S.; Tomasi, J.; Cossi, M.; Rega, N.; Millam, J. M.; Klene, M.; Knox, J. E.; Cross, J. B.; Bakken, V.; Adamo, C.; Jaramillo, J.; Gomperts, R.; Stratmann, R. E.; Yazyev, O.; Austin, A. J.; Cammi, R.; Pomelli, C.; Ochterski, J. W.; Martin, R. L.; Morokuma, K.; Zakrzewski, V. G.; Voth, G. A.; Salvador, P.; Dannenberg, J. J.; Dapprich, S.; Daniels, A. D.; Farkas, O.; Foresman, J. B.; Ortiz, J. V.; Cioslowski, J.; Fox, D. J. *Gaussian 09*, revision D.01; Gaussian Inc., 2009.
(53) Hino, J. K.; Della Ciana, L.; Dressick, W. J.; Sullivan, B. P. Substituent constant correlations as predictors of spectroscopic, electrochemical, and photophysical properties in ring-substituted 2,2′-bipyridine complexes of rhenium(I). *Inorg. Chem.* **1992**, *31*, 1072.
(54) Lu, T.; Chen, F. Multiwfn: A multifunctional wavefunction analyzer. *J. Comput. Chem.* **2012**, *33*, 580.
(55) Hamm, P.; Lim, M.; Hochstrasser, R. M. Vibrational energy relaxation of the cyanide ion in water. *J. Chem. Phys.* **1997**, *107*, 10523.
(56) Hamm, P.; Kaindl, R. A.; Stenger, J. Noise suppression in femtosecond mid-infrared light sources. *Opt. Lett.* **2000**, *25*, 1798.
(57) Helbing, J.; Hamm, P. Compact implementation of Fourier transform two-dimensional IR spectroscopy without phase ambiguity. *J. Opt. Soc. Am. B* **2011**, *28*, 171.
(58) Sato, S.; Matubara, Y.; Koike, K.; Falkenström, M.; Katayama, T.; Ishibashi, Y.; Miyasaka, H.; Taniguchi, S.; Chosrowjan, H.; Mataga, N.; Fukazawa, N.; Koshihara, S.; Onda, K.; Ishitani, O. Photochemistry of *fac*-$[Re(bpy)(CO)_3Cl]$. *Chem. - Eur. J.* **2012**, *18*, 15722.
(59) Bredenbeck, J.; Helbing, J.; Hamm, P. Continuous scanning from picoseconds to microseconds in time resolved linear and nonlinear spectroscopy. *Rev. Sci. Instrum.* **2004**, *75*, 4462.
(60) Shillito, G. E.; Hall, T. B.; Preston, D.; Traber, P.; Wu, L.; Reynolds, K. E.; Horvath, R.; Sun, X. Z.; Lucas, N. T.; Crowley, J. D.; George, M. W.; Kupfer, S.; Gordon, K. C. Dramatic Alteration of ^{3}ILCT Lifetimes Using Ancillary Ligands in $[Re(L)(CO)_3(phen-TPA)]^{n+}$ Complexes: An Integrated Spectroscopic and Theoretical Study. *J. Am. Chem. Soc.* **2018**, *140*, 4534.
(61) Kumar, A.; Sun, S.-S.; Lees, A. J. Photophysics and Photochemistry of Organometallic Rhenium Diimine Complexes. In *Photophysics of Organometallics*; Lees, A. J., Ed.; Springer: Berlin, 2010; pp 37−71.
(62) Johnson, F. P. A.; George, M. W.; Hartl, F.; Turner, J. J. Electrocatalytic Reduction of CO_2 Using the Complexes $[Re(bpy)(CO)_3L]^n$ (n = + 1, L = $P(OEt)_3$, CH_3CN; n = 0, L = Cl^-, Otf^-; bpy = 2,2′-Bipyridine; Otf^- = CF_3SO_3) as Catalyst Precursors: Infrared Spectroelectrochemical Investigation. *Organometallics* **1996**, *15*, 3374.
(63) Probst, B.; Kolano, C.; Hamm, P.; Alberto, R. An efficient homogeneous intermolecular rhenium-based photocatalytic system for the production of H_2. *Inorg. Chem.* **2009**, *48*, 1836.
(64) Probst, B.; Rodenberg, A.; Guttentag, M.; Hamm, P.; Alberto, R. A highly stable rhenium-cobalt system for photocatalytic H_2 production: Unraveling the performance-limiting steps. *Inorg. Chem.* **2010**, *49*, 6453.
(65) Bachmann, C.; Probst, B.; Guttentag, M.; Alberto, R. Ascorbate as an electron relay between an irreversible electron donor and Ru(II) or Re(I) photosensitizers. *Chem. Commun.* **2014**, *50*, 6737.
(66) Horváth, A.; Stevenson, K. L. Transition metal complex exciplexes. *Coord. Chem. Rev.* **1996**, *153*, 57.
(67) Vogler, A.; Kunkely, H. Charge transer exciplex emission involving a transition metal complex. *Inorg. Chim. Acta* **1980**, *45*, L265.

https://dx.doi.org/10.1021/acs.inorgchem.0c01939
Inorg. Chem. XXXX, XXX, XXX−XXX